The Plant Journal (2001) **26**(3), 249–264

The shoot apical meristem restores its symplasmic organization during chilling-induced release from dormancy

Päivi L. H. Rinne[1,†], Päivi M. Kaikuranta[1] and Christiaan van der Schoot[2,3,*]
[1]*Department of Biology, University of Oulu, PO Box 3000, FIN-90014 Oulu, Finland,*
[2]*ATO, Wageningen University and Research Centre, Bornsesteeg 59, PO Box 17, NL-6700 AA Wageningen, The Netherlands, and*
[3]*Department of Biology and Nature Conservation, Plant Developmental Physiology, Agricultural University of Norway, PO Box 5014, N-1432 Ås, Norway*

Received 27 November 2000; revised 13 February 2001; accepted 16 February 2001.
[*]For correspondence (fax +47 649 48502; e-mail chris.vanderschoot@ibn.nlh.no).
[†]Present address: Department of Biology and Nature Conservation, Plant Developmental Physiology, Agricultural University of Norway, PO Box 5014, N-1432 Ås, Norway.

Summary

The shoot apex of overwintering perennials ceases its morphogenetic activity at the end of the growing season and transforms into a bud which is dormant and freezing-tolerant. In birch (*Betula pubescens*) these events are triggered by short photoperiod, and involve the production of 1,3-β-D-glucan containing sphincters on the plasmodesmata. As a result, all symplasmic pathways shut down. Here we show that breakage of bud dormancy by chilling involves restoration of the symplasmic organization of the meristem. This restoration is likely to be mediated by 1,3-β-D-glucanase, which was present in small spherosome-like vacuoles that arose *de novo* during dormancy induction. During chilling these vacuoles were displaced from the bulk cytoplasm to the cortical cytoplasm where they became aligned with the plasma membrane, often associated with plasmodesmata. At this stage the enzyme also appeared outside the vacuoles. During chilling, 1,3-β-D-glucan disappeared from the plasmodesmal channels and wall sleeves, and the plasmodesmata regained the capacity for cell–cell transport, as demonstrated by microinjection of Lucifer Yellow CH and Fluorescein-tagged gibberellic acid. Collectively, the present experiments demonstrate that restoration of the symplasmic organization of the meristem is indispensable for the release of buds from dormancy and the assumption of a proliferation-competent state, and implicate 1,3-β-D-glucanase action at the plasmodesmata. Based on these findings we propose a model for 'dormancy cycling' which depicts the meristem as passing through three sequential states of cellular communication with characteristic sensitivities to distinct environmental cues.

Keywords: dormancy, 1,3-β-D-glucanase, plasmodesmata, shoot apical meristem, spherosome, cell–cell communication.

Introduction

Perennial plants of the temperate zones have developed unique mechanisms to anticipate the regular environmental changes that occur during the progression of the seasons. For example, at the end of the growing season they cease development and assume a dormant and freezing-tolerant state even when temperatures still favour growth, a strategy that protects against a sudden arrival of winter. Later in winter they may already anticipate spring by breaking dormancy while freezing tolerance remains high (Weiser, 1970). This synchrony of growth with the seasons – referred to as 'dormancy cycling' – has received considerable attention, but the underlying mechanisms have remained unresolved for buds (Lang, 1994; Lang, 1996) as well as for seeds (Bewley, 1997).

In order to cease growth and assume dormancy in a timely fashion, perennials often measure the length of the photoperiod by means of phytochromes (Hauser *et al.*, 1998; Vegis, 1964; Vince-Prue, 1994). The phytochromes shuttle between the cytoplasm and the nucleoplasm (Kircher *et al.*, 1999; Yamaguchi *et al.*, 1999) and generate

a putative signal (or set of signals) that is sent out from the leaves, via the petioles and the stem, towards the shoot apex (Vince-Prue, 1994). The shoot apex, as the actual target of the signal, responds by transforming itself into a dormant bud. Often the dormant bud regains the potential for further growth and development only after it has received adequate exposure to cold (Noodén and Weber, 1978; Powell, 1987). This so-called 'chilling requirement' is widespread, not only in the case of vegetative buds but also in floral buds, where it is known as vernalization (Gassner, 1918; cited in Salisbury and Ross, 1992). Several studies have shown that it is the bud itself, vegetative or floral, which must be exposed to low temperatures (Metzger, 1996 and references therein); chilling of the plant body alone is insufficient. This is important as it shows that the bud cannot import the effect of chilling from the rest of the plant. It also implies that dormancy release is based on processes that are intrinsic to the bud itself (Metzger, 1996). In support of this idea, studies with seeds have shown that chilling directly affects the apical meristem (AM), since a dormant AM isolated from the embryo can be released from dormancy by chilling (Metzger, 1988; Purvis, 1940; Purvis, 1961). In conclusion, it is plausible that the AM, inside the bud or apex is the central player in all phases of dormancy cycling.

Studies on the hormonal control of dormancy suggest that gibberellic acid (GA) is closely involved in the chilling-induced release of buds from dormancy. For example, early work showed that application of GA to a dormant bud can break dormancy (Walker and Donoho, 1959), indicating that GA can somehow substitute for chilling. Measurements of endogenous GA, for example in apple seeds (Bianco *et al.*, 1984), have shown that chilling can actually elevate GA levels by stimulating GA biosynthesis (Hazebroek *et al.*, 1993; Powell, 1987; Zanewich and Rood, 1995). However, GA application is not the only way to break dormancy experimentally. Many abiotic factors may suffice, such as anaerobiosis, freezing, high temperature, and a range of different chemicals (Cohn, 1996; Rinne *et al.*, 1997; Shirazi and Fuchigami, 1995; Tanino *et al.*, 1989; Wisniewski *et al.*, 1996). The fact that such a wide variety of factors can break dormancy brings into question the existence of universal key components and pathways in dormancy cycling, as well as the validity of existing theories and concepts (Lang, 1987).

As multiple effectors may lead to dormancy breaking, the process is unlikely to be reliant on a linear control pathway. Rather, it may depend on the collective behaviour of interconnected metabolic pathways. At the cellular level the activation of individual pathways may then result in canalization towards an identical cell state (van der Schoot, 1996). This may be true not only for intracellular, but also for intercellular networks, that is, those that function at the level of the integrated AM (van der Schoot, 1996). From this perspective, dormancy cycling can be investigated in terms of changes in cell–cell networking at the AM (van der Schoot and Rinne, 1999a; van der Schoot and Rinne, 1999b).

In the first stage, when the AM is active in morphogenesis, cell–cell signalling networks are positioned and interconnected in such a way that they support the formation of essential patterns (Crawford and Zambryski, 1999; Laufs *et al.*, 1998a; Laufs *et al.*, 1998b; Lenhard and Laux, 1999; Meyerowitz, 1999; Rinne and van der Schoot, 1998; van der Schoot, 1996; Vernoux *et al* 2000; van der Schoot and Rinne, 1999b). The symplasmic part of this network – which complements the membrane-based signalling systems – is created by plasmodesmata that interconnect all the cells of the AM. This symplasmic space provides a direct route for cell–cell signalling (Bergmans *et al.*, 1993, Bergmans *et al.*, 1997; Lucas *et al.*, 1993; McLean *et al.*, 1997). Borders at particular locations – between AM centre and periphery, and between tunica and corpus – prevent the free diffusion of signals across the symplasmic field boundaries, thereby creating developmental zones with distinct tasks (Crawford and Zambryski, 1999; Gisel *et al.*, 1999; Rinne and van der Schoot, 1998; van der Schoot and Rinne, 1999a; van der Schoot and Rinne, 1999b).

In perennials like birch the AM enters a second stage during dormancy induction, in which symplasmic pathways are shut down by the formation of pronounced 1,3-β-D-glucan containing sphincters on all plasmodesmata. As a result, symplasmic communication is suspended and the functioning of the AM as an integrated whole is prevented. Local activation of 1,3-β-D-glucan synthase complexes is therefore a crucial step in the establishment of dormancy (Rinne and van der Schoot, 1998).

We hypothesized that in the third stage, when the AM is released from dormancy, the reverse process may be required, that is, breakdown of plasmodesmal 1,3-β-D-glucan complexes. The present experiments provide evidence that chilling restores the symplasmic organization of the birch AM by enhancing the production of 1,3-β-D-glucanases as well as the delivery of preproduced 1,3-β-D-glucanases in spherosome-like vacuoles into the vicinity of the plasmodesmata. As a result 1,3-β-D-glucan is gradually removed from the plasmodesmal sphincter ring and the plasmodesmal channel. We further demonstrate with microinjection experiments that the biochemical modifications of plasmodesmata underlie the symplasmic restoration of the AM. The present experiments show for the first time that during dormancy cycling, precisely timed symplasmic alterations occur in the AM that affect the capacity of the AM cells to symplastically exchange metabolites, small signalling molecules and hormones. Based on these as well as earlier findings (Rinne and van der Schoot, 1998), we present a model of dormancy

cycling that depicts the AM as passing through three sequential states of cellular communication – online, offline and standby – each being selectively responsive to environmental factors that evoke the transition to the next state.

Results

Separating dormancy from freezing tolerance

Birch (*Betula pubescens*) develops dormancy as well as freezing tolerance in response to a photoperiod that is shorter than a critical value (approximately 16 h for the ecotype studied). We were particularly interested in those changes in the AM that are crucial and characteristic of the dormant state. As both dormancy development and freezing tolerance might alter the functional structure of the AM, we first investigated if and how they could be experimentally separated. By using a set of controlled regimes we found conditions under which dormancy was adequately disconnected from freezing tolerance (Figure 1).

Under a long photoperiod, the seedlings elongated steadily and formed leaves at regular intervals (plastochron index 0.5). Transfer to short photoperiod at room temperature resulted within 4–6 days in an arrest of leaf initiation (inside the apex), while shoot elongation ceased 2–3 days later. This development towards dormancy appeared to be reversible by return to long photoperiod during the first 2 weeks. After this 2-week period dormancy became established (fixed), and an adequate exposure to chilling was necessary to break it (Figure 1). For the sake of convenience we refer to this phase of fixed dormancy simply as 'dormancy', which corresponds to endodormancy (Romberger, 1963) and deep or true dormancy (Lang, 1987).

Transfer of seedlings to short photoperiod at room temperature was also sufficient to develop freezing tolerance. The first increase in freezing tolerance could already be measured after 3 weeks under short photoperiod, but a maximum tolerance level of –20°C required 7 weeks to develop (Figure 1). A subsequent 6-week chilling period (2°C) increased the freezing tolerance beyond –70°C, but removed dormancy, that is, it restored the ability of the AM to proliferate under forcing conditions (Figure 1). We refer to this post-dormant but inactive state of the AM as either 'ecodormant' (Romberger, 1963) or 'released', as the AM is no longer intrinsically dormant but is only kept inactive by external conditions that are incompatible with growth.

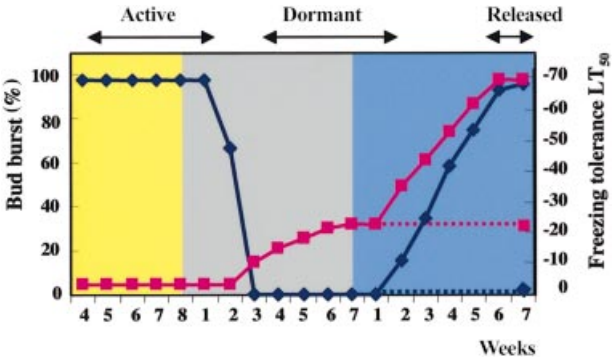

Figure 1. Separation of dormancy and freezing tolerance in birch (*Betula pubescens*) under controlled regimes.
The actively growing plants at long photoperiod (yellow) have axillary buds that are resting. They are not dormant, however, as about 100% of them were able to burst (blue line) when the stem was cut into single-nodes and grown in water culture under growth-promoting conditions. These potentially active buds lacked freezing tolerance (red line). When the plants were exposed to a short photoperiod (grey) for 3 weeks, they became entirely dormant, that is, buds no longer burst under growth-promoting conditions. At this stage freezing tolerance was initiated, and it reached –20°C (LT_{50}) in 7 weeks. The dormant buds were released from dormancy only if they were exposed to chilling at 2°C (blue). While chilling removed dormancy in approximately 6 weeks, it further deepened freezing tolerance to a new maximum (LT_{50} –70°C). Without chilling, after an identical period under short photoperiod, buds remained dormant (blue stippled line) and did not develop freezing tolerance further (red stippled line). Numbers under the diagram indicate the duration of the applied regimes. Arrows at the top of the diagram indicate the three developmental stages of the apical meristem (active, dormant and released) that were used in further investigations.

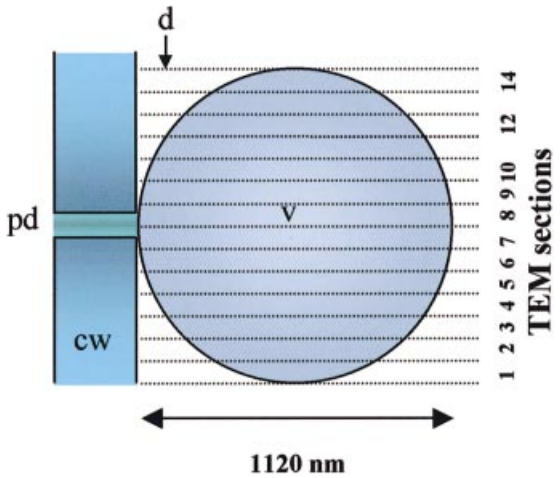

Figure 3. Schematic illustration of the alignment between a spherical vacuole and a plasmodesma in 14 successive TEM sections.
In most sections (80 nm) the vacuole (v, diameter 1120 nm) appears at a certain distance (d) from the cell wall (between 0 and 350 nm). Due to the small dimensions of plasmodesmata (pd, 80–100 nm), only one or two median sections of the vacuole can show a connection to it (7 or 14% of all the sections, respectively). In TEM sections of the birch apical meristem, approximately 7% of all cortical spherosome-like vacuoles were observed to touch places where plasmodesmata cross the wall, which implies roughly half of them may actually touch the plasmodesmata.

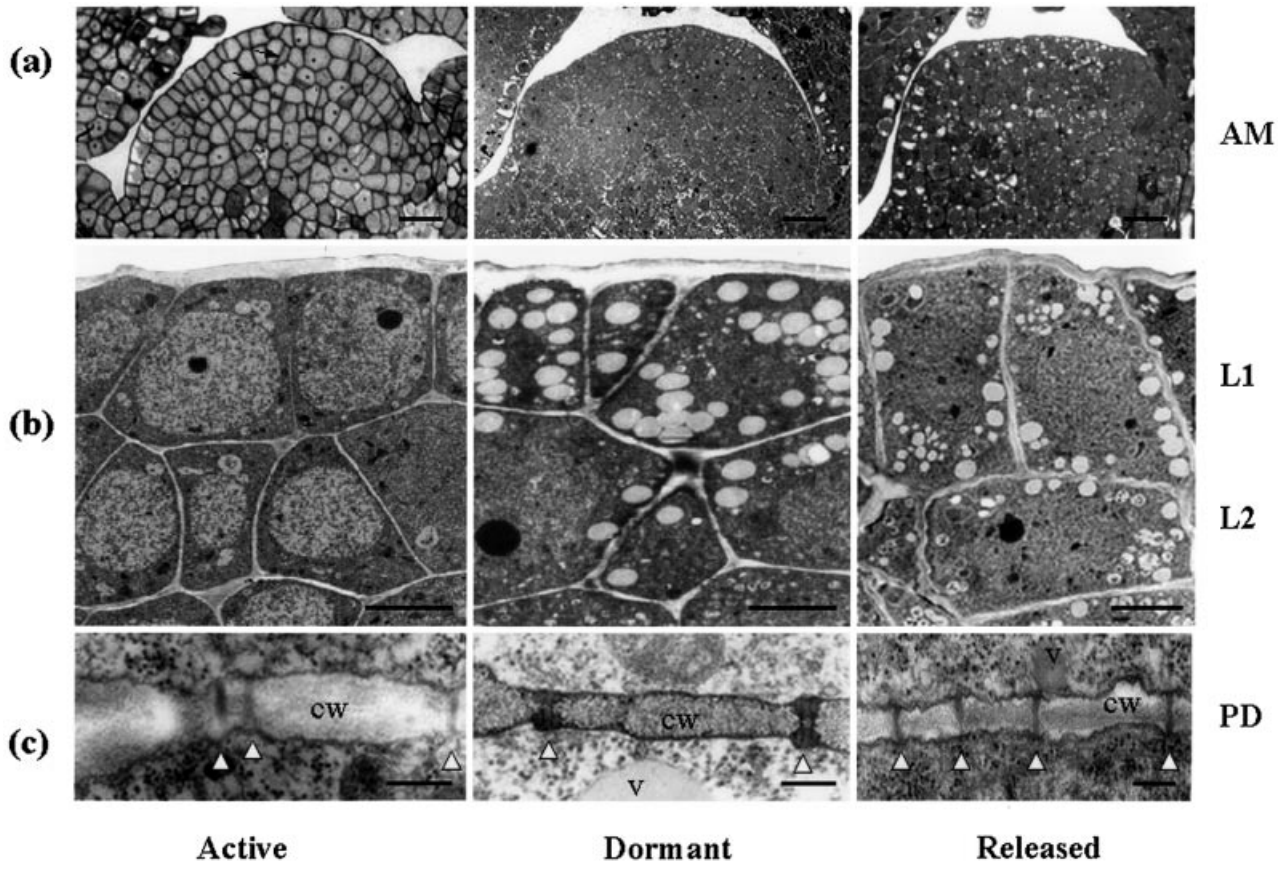

Figure 2. Cytological and ultrastructural changes in apical meristems of birch (*Betula pubescens*) during dormancy cycling.
(a) Overview of the apical meristem (AM) in median longitudinal sections. In the active AM, cells are continuously dividing (arrows indicate typical division walls). The cell walls are thin and stain strongly. During dormancy development, cell divisions are no longer apparent. Numerous small vacuoles appear (small translucent spots) that remain present throughout the phase of dormancy release until growth commences. The cell walls are thickened and stain lightly in dormant and released AM.
(b) Location of small vacuoles in AM cells (shown here for the two uppermost cell layers, L_1 and L_2, at the central part of the AM). The few vacuoles in cells of the active AM are commonly close to the nucleus, whereas the uniformly sized vacuoles (spherosome-like) in the dormant AM are dispersed throughout the cytoplasm. During dormancy release these vacuoles are crowding at the peripheral part of the cytoplasm at the cell wall and plasma membrane.
(c) Presence of sphincters at plasmodesmal entrances, here shown for the interface between L_1 and L_2. Arrowheads indicate plasmodesmata. In the active AM no plasmodesmal sphincters are visible, whereas in the dormant AM all plasmodesmal entrances are equipped with electron-dense sphincters. In the released but non-proliferating AM (ecodormant), plasmodesmal sphincters are no longer apparent. To enhance the contrast of membranes and plasmodesmata, the fixation of all apices was carried out with osmium tetroxide (1% w/v) and tannic acid (1% w/v) in the fixation medium. The imposed regimes for the three AM stages are indicated in Figure 1. Scale bars: (a) 25 μm; (b) 5 μm; (c) 250 nm. cw, cell wall; v, vacuole.

Table 1. Distribution of 1,3-β-D-glucanase containing spherosome-like vacuoles in cells of dormant and released meristems

Distance from cell wall (nm)	Dormant[a] (%)	Released[b] (%)
0 (at plasmodesmata)[c]	–	7.0
<200[c]	21.8	49.5
200–350[c]	22.5	27.0
350–500	22.2	9.3
>500	33.5	7.2

[a]275 vacuoles;

Table 2. The average number of gold particles at plasmodesmata (PD) in active, dormant and released apical meristems (AM)

AM status	Number of gold particles (SE)[a]	Number of AM (PD)
Active	1.0 (0.3)	3 (580)
Dormant	5.5 (1.1)	3 (324)
Released	2.0 (0.2)	3 (250)

[a]ANOVA indicates values are significantly different. SE, standard error.

Vacuoles and plasmodesmal structures during dormancy cycling

Exposure of the plants to short photoperiod gave rise to some prominent changes in the AM that appeared to be characteristic of the dormant state. The cell walls showed reduced staining capacity (Methylene Blue, Azure and Basic Fucsin, see Experimental procedures) indicating that the cell-wall properties change when the AM switches to a dormant state (Figure 2a). Large numbers of small, translucent vacuoles appeared in all cells (Figure 2a). Owing to the relatively uniform size of the vacuoles, between 0.5 and 2 μm, their translucent nature in the electron microscope, and the presence of an apparent 'half-unit' membrane, they resembled the lipid containing spherosomes described for a variety of plant systems (Matile, 1975). Because they also contain proteins, we refer to them tentatively as 'vacuoles' or 'spherosome-like vacuoles'. However, they were different from the protein-storage vacuoles that were situated closer to the nucleus (Rinne *et al.*, 1999). The electron translucent vacuoles were scattered throughout the cytoplasm in the dormant AM, whereas in chilled meristems they were crowded in the cortical cytoplasm (Figure 2b). Measurements confirmed that at this stage the majority of the spherosome-like vacuoles were in close proximity to the plasma membrane (on average within 350 nm), and 7% of them appeared in sections to be in direct association with plasmodesmata (Table 1). Due to the small transverse dimensions of plasmodesmata (80–100 nm), and the fact that vacuoles are spheres that touch the plasma membrane only tangentially, the association is likely to be seen only in two median sections of each vacuole. For example, in a vacuole of 1.12 μm they would represent 14% of the total number of sections through the vacuole (Figure 3). In that case, an observation of 7% would imply that half of the vacuoles actually touch the plasmodesmata. At present it suffices to conclude that a substantial number of vacuoles contacts the plasmodesmata. Examination of serial sections supported this conclusion, that is, vacuoles that did not touch the cell membrane and plasmodesmata in a given section often did so in subsequent sections (not shown).

Significant alterations took place in the morphology and substructure of the plasmodesmata during the AM transitions. In contrast to the actively proliferating AM, the

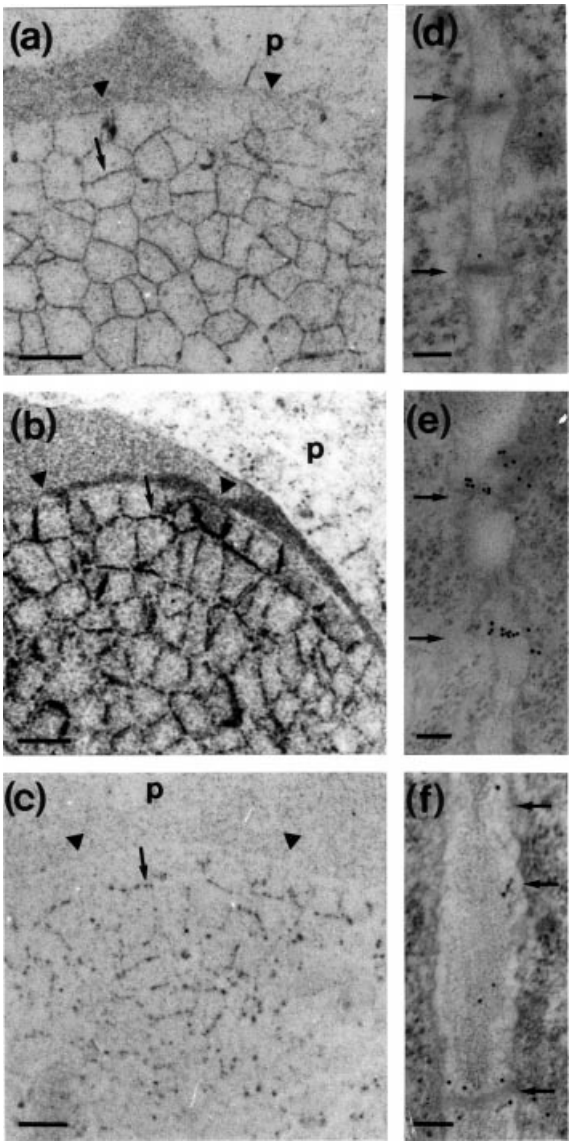

Figure 4. Immunolocalization of 1,3-β-D-glucan in the shoot apical meristem (AM) of birch (*Betula pubescens*) during dormancy cycling.
Micrographs of medium longitudinal sections through apical meristems (a–c) and TEM micrographs of their plasmodesmata (d–f). Note that in (a–c) immunogold labelling is silver-enhanced (grey to black precipitation at immunoreactive areas) and the sections lack counterstaining, and that in (d–f) 10 nm gold particles indicate the specific location of the antigen in sections that are counterstained.
(a) Active AM. Silver precipitation was present as a thin but continuous lining of the young cell walls (grey; arrow) indicating that some 1,3-β-D-glucan was present in the cell walls.
(b) Dormant AM. Silver precipitation appeared in a pronounced dotted (black) pattern at the cell walls (arrow) indicating high amounts of 1,3-β-D-glucan locally at the cell walls.
(c) Released but non-proliferating AM (ecodormant). Silver precipitation appeared in a punctuated pattern, but was less intense (grey) than in (b).
(d) Detail of a typical cell-wall interface in (a). Plasmodesmata (arrows) and cell walls possess only few gold particles.
(e) Detail of a typical cell-wall interface in (b). Plasmodesmata (arrows) show extensive labelling at the sphincter ring and at the channel. The sphincter ring itself is invisible due to the absence of tannic acid in the fixation medium because of immunolabelling requirements.
(f) Detail of a typical cell-wall interface in (c). Plasmodesmata (arrows) do not show labelling of the channel, but some gold particles are present at the cell-wall sleeve surrounding the plasmodesmata.
The imposed regimes for the three AM stages are indicated in Figure 1. Arrowheads (a–c) point to the outer cell layer of the AM. Scale bars: (a–c) 15 μm; (d–f) 100 nm; p, primordia.

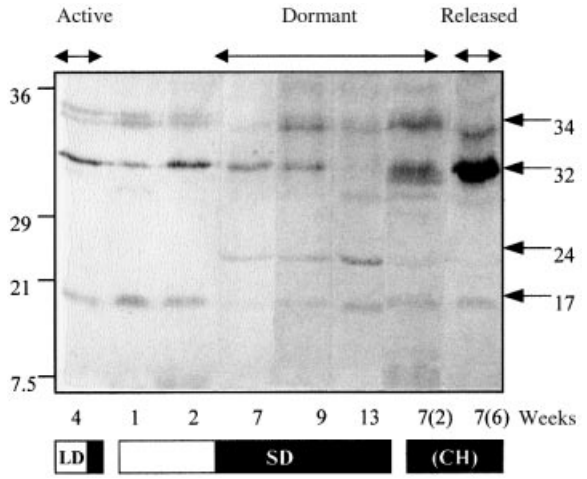

Figure 5. Production of 1,3-β-D-glucanases in the AM of birch (*Betula pubescens*) during dormancy cycling as analysed by Western blots.
Equal amounts of protein (10 μg) were loaded in each well. Molecular weights (M_w) of protein markers are shown on the left in kilodaltons. The arrows on the right indicate the proteins that were detected with antibody against 1,3-β-D-glucanase. The duration of treatments (long and short days [LD, SD] and chilling [CH]) is indicated in weeks (for chilling in parenthesis; the first 7 weeks were always under short photoperiod). The imposed regimes for the three AM stages are indicated in Figure 1.

dormant AM possessed sphincters at the entrances of all plasmodesmata (Figure 2c). The plasmodesmal channel appeared normal in size, however. The sphincters became visible by use of tannic acid in the fixative, revealing the presence of proteinaceous substances at these areas. Without tannic acid the sphincter areas appeared as relatively translucent spots. Chilling of dormant plants for 6 weeks, which suffices to release them from dormancy, restored the normal morphology of the plasmodesmata (Figure 2c).

Localization of 1,3-β-D-glucan during dormancy cycling

Previously we have shown that in the dormant AM the sphincters contain pronounced deposits of 1,3-β-D-glucan, whereas the surrounding cell-wall areas are virtually devoid of it (Rinne and van der Schoot, 1998). Here we have systematically investigated the overall pattern of 1,3-β-D-glucan depositions under various environmental conditions by using immunocytochemistry at light microscope level (LM) (Figure 4a–c). We found that in the actively growing AM, some 1,3-β-D-glucan was consistently present at the forming cell plates as well as at the cell walls, although in a very thin and continuous layer (Figure 4a). In contrast, in the dormant AM anti-1,3-β-D-glucan-antibody was present at all cell walls in a pronounced, dotted pattern (Figure 4b), suggesting the presence of substantial 1,3-β-D-glucan deposits at the individual plasmodesmata. After a chilling period that was sufficient to remove dormancy, the 1,3-β-D-glucan depositions were strongly reduced in the entire AM and could even be absent in the anticlinal walls of the tunica (Figure 4c). The dotted pattern could still be discerned, however. The

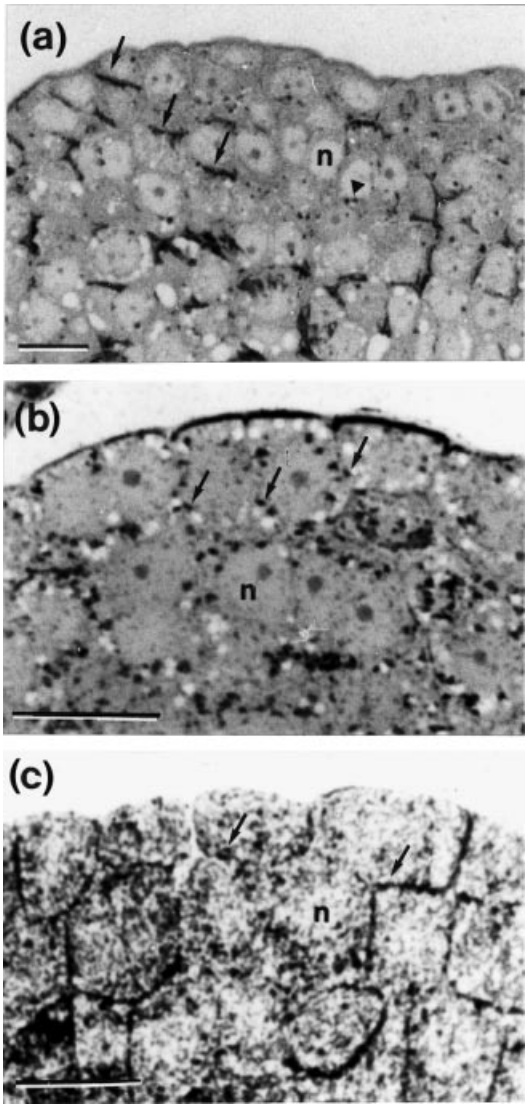

Figure 6. Immunolocalization of 1,3-β-D-glucanase in the apical meristem (AM) of birch (*Betula pubescens*) during dormancy cycling at the light-microscope level.
(a) Active AM. Silver-enhanced immunogold label (black) is detected predominantly at forming cell plates – where 1,3-β-D-glucanases are active in the removal of cell-plate 1,3-β-D-glucan (arrows) – and in the few vacuoles that are present at this stage (arrowhead). Counterstained with toluidine blue (1% w/v).
(b) Dormant AM. Silver precipitation (black) indicates the presence of 1,3-β-D-glucanases in the numerous small vacuoles (black) that appear at this stage (arrows). Counterstained with toluidine blue (1% w/v).
(c) Released but non-proliferating AM (ecodormant). Silver precipitation (black) suggests that 1,3-β-D-glucanase is present both in spherosome-like vacuoles and free in the cytoplasm, particularly at the cortical area (arrows). No counterstaining.
The imposed regimes for the three AM stages are indicated in Figure 1. Scale bars: 10 μm; n, nucleus.

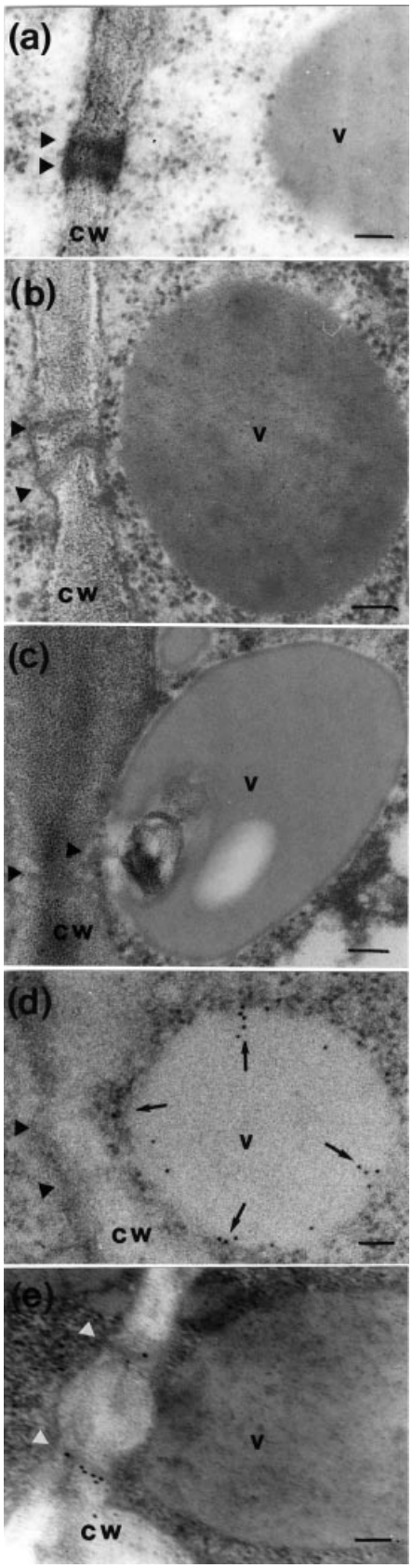

controls were free of label (normal serum and irrelevant antibodies; not shown). The presence of 1,3-β-D-glucan deposits as described above was further confirmed by localization experiments at the transmission electron microscope (TEM) level (Figure 4d–f). In the dormant AM the plasmodesmal channels and sphincter rings were labelled with anti-1,3-β-D-glucan-antibody (Figure 4e), whereas in the active (Figure 4d) as well as in the released AM (Figure 4f) some label was occasionally present in the wall, particularly at the sleeve around the plasmodesmata, but not in the plasmodesmal channel itself. Gold label counts, performed on TEM sections, showed that the dormant AM possessed significantly higher amounts of 1,3-β-D-glucan at the plasmodesmata than the ecodormant and active AM (Table 2).

Production and localization of 1,3-β-D-glucanases during dormancy cycling

As chilling resulted in the disappearance of 1,3-β-D-glucan at the entrances of the plasmodesmata, we further investigated whether the chilling effect was mediated by the 1,3-β-D-glucan-degrading enzyme 1,3-β-D-glucanase. In Western blot analysis the antibody against 1,3-β-D-glucanase revealed that the common 1,3-β-D-glucanases (32 and 34 kDa) were continuously present in the meristem regardless of phase of dormancy cycle (Figure 5). The same antibody also cross-reacted with a 17- and a 24-kDa protein, the identity of which remains to be established. Interestingly, however, the 24-kDa protein appeared only in the dormant AM at the point where return to favourable

Figure 7. Association of 1,3-β-D-glucanase containing spherosome-like vacuoles (spherosomes) with plasmodesmata in the AM of birch (*Betula pubescens*) during chilling-induced dormancy release.
(a) Dormant AM after 2 weeks of chilling. Dormancy is not yet broken and sphincters remain present at the plasmodesmata (arrowheads). Small vacuoles (v) are typically present at some distance from the cell walls (cw).
(b) Released AM (after 6 weeks of chilling). Vacuoles (v) are typically in close proximity to the cell walls and partly associated with plasmodesmata (arrowheads), which at this point have lost their prominent sphincters.
(c) Released AM. Vacuoles (v) that touch plasmodesmata (arrowheads) sometimes engulf membranous structures that may have been covering the sphincter ring. Note that the plasmodesmata are obliquely cut.
(d) Released AM. Immunogold labelling of 1,3-β-D-glucanase at the ultrastructural level indicates that the enzyme is present (arrows) in the peripheral part of the vacuoles (v), allowing close contact with the plasmodesmata (arrowheads).
(e) Released AM. Immunogold labelling of 1,3-β-D-glucan at the ultrastructural level indicates that the remaining substrate for 1,3-β-D-glucanase is at the plasmodesmal wall sleeve (arrowheads), but not in the channel.
Fixation is carried out with osmium tetroxide (1% w/v) and tannic acid (1% w/v) except for (d,e) where the contrast of plasmodesmal structure is reduced. Imposed regimes for the AM stages are indicated in Figure 1. Scale bars: (a) 200 nm; (b–e) 100 nm; cw, cell wall; v, vacuole (spherosome-like).

conditions no longer sufficed to promote regrowth. This band disappeared when the AM was released from dormancy, while a 32-kDa 1,3-β-D-glucanase became considerably upregulated.

We next addressed the question of at which cellular sites 1,3-β-D-glucanase is present in these distinct phases. Silver-enhanced immunogold labelling confirmed that 1,3-β-D-glucanase was indeed localized in patterns that were different for each phase of the dormancy cycle (Figure 6). In the active AM, the enzyme was predominantly present at forming cell plates and young division walls. Localization in small vacuoles was found occasionally (Figure 6a). In the dormant AM, however, the antibody against 1,3-β-D-glucanase was localized only in the

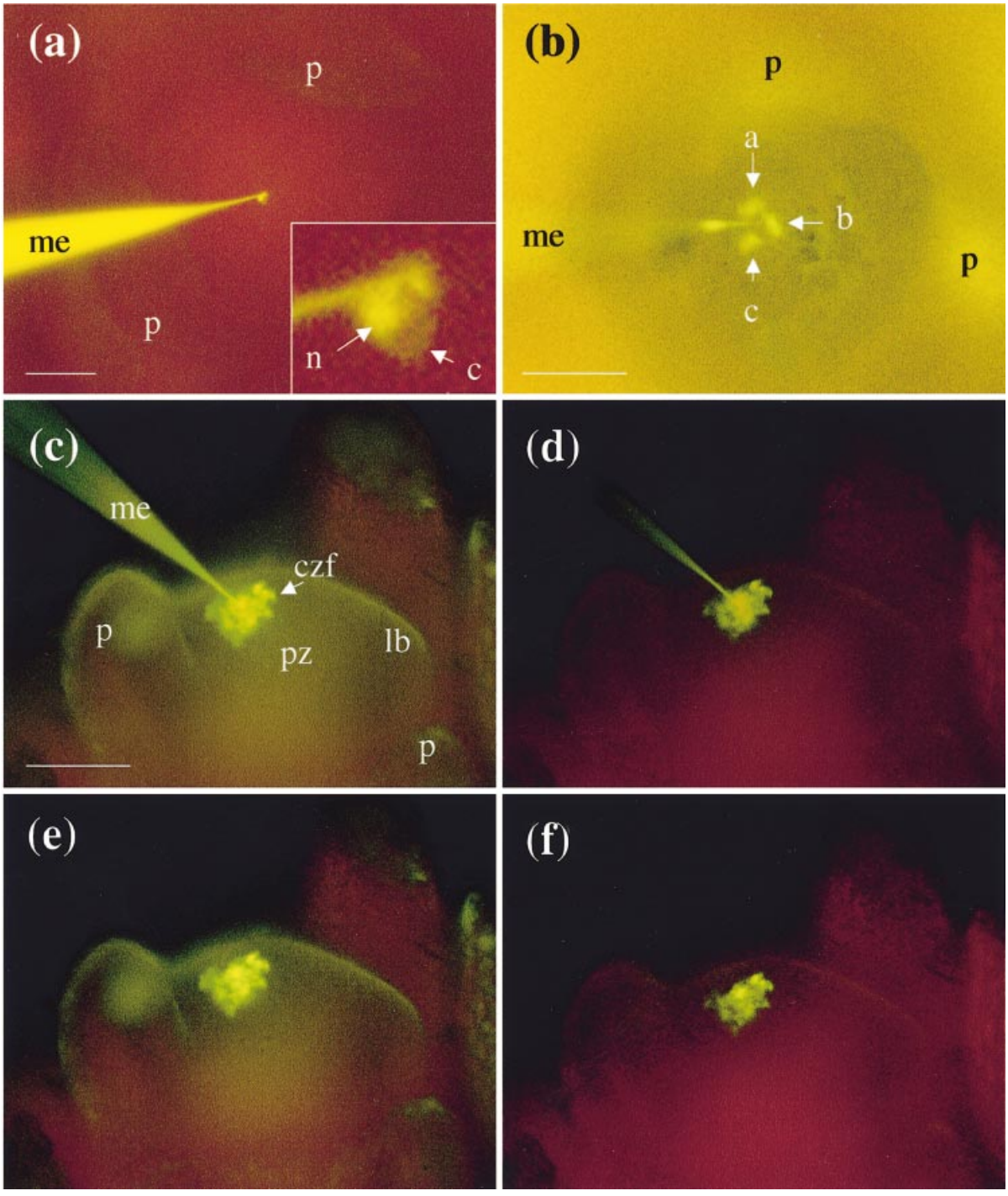

spherosome-like vacuoles (Figure 6b) that were formed abundantly in response to short photoperiod. We did not detect any 1,3-β-D-glucanase in patterns reminiscent of cell plates in the dormant AM, which is expected in view of the virtual absence of mitotic activity in the dormant state. When the dormant AM had been exposed to chilling, the 1,3-β-D-glucanase-containing vacuoles were commonly in close proximity to the cell walls, although the enzyme also appeared in a more-or-less continuous lining of the cell walls (Figure 6c).

Ultrastructural investigations showed that the spherosome-like vacuoles, which often became associated with plasmodesmata during chilling (Figure 7a–c), typically contained 1,3-β-D-glucanase peripherally in their lumen (Figure 7d). Some of these vacuoles appeared to be integral parts of a cortical ER network – which itself could contain some 1,3-β-D-glucanase (not shown) – explaining the more-or-less continuous lining of silver precipitate at the cell-wall area at the LM level (Figure 6c). The fact that 1,3-β-D-glucan disappeared from the channels (Figure 7e; Table 2) during the period when the vacuoles were present at the plasmodesmata or in close proximity to it (Table 1) suggests that these spherosome-like vacuoles and/or ER somehow deliver the hydrolytic enzymes to the 1,3-β-D-glucan deposits at the plasmodesmal neck and channel. Although present at the plasmodesmal entrances, 1,3-β-D-glucanase was seldom detected precisely inside the sphincters or inside the channel of the plasmodesmata (Figure 7d).

Alterations in cell–cell communication during dormancy cycling

Having established that alterations of plasmodesmal morphology, substructure and composition closely corresponded to the various phases of dormancy cycling, we addressed the question as to whether this also implies that the plasmodesmata are functionally altered. To test this, we used an iontophoretic microinjection technique by which fluorescent dyes or fluorescently labelled molecules were introduced into single AM cells. In the actively proliferating AM (Rinne and van der Schoot, 1998), the membrane-impermeant fluorescent dye Lucifer Yellow CH (LYCH) diffused through plasmodesmata from cell to cell, whereas in the dormant AM such cell–cell transport was absent after 4 days under short photoperiod (Figure 8a). After a chilling period of more than 3 weeks, AM cells occasionally transported LYCH to a few neighbouring cells. These scant dye-coupling groups appeared to be fragments of the future symplasmic fields. Only after a 6-week chilling period were the AM cells correctly re-assembled into dye-coupling patterns similar to those found in actively proliferating meristems (Figure 8c–f).

Identical microinjection experiments were carried out with the plant hormone gibberellic acid (GA_4), which is thought to play a role in chilling-induced dormancy release. To monitor a possible cell–cell movement, we used fluorescently tagged GA_4 (F-GA_4). The GA_4 was labelled with Fluorescein at the 16(17)-double bond, where chemical modification usually does not affect biological activity (Pulici *et al.*, 1996). A mercaptoalkylthio group was present as a spacer between the fluorescent group and the GA moiety to allow interaction between the latter and the putative receptor (Pulici *et al.*, 1996). Experimentally, we first examined whether the F-GA_4 could move from cell to cell in the AM via the plasmodesmata, and secondly if it could advance the observed opening of the plasmodesmata during chilling. When F-GA_4 was microinjected into a single cell of a 6-week-chilled AM (released or ecodormant), it moved to all cells in the AM centre in patterns similar to those found for LYCH (Figure 9). However, microinjection of F-GA_4 into single cells of the dormant AM did not result in any movement within a time frame of 6 h (Figure 8b).

Discussion

The functioning of the AM is based on coherent and robust patterns of cell–cell communication. The integrated communication network of the AM partly resides in the

Figure 8. Cell–cell communication in the shoot apical meristem (AM) of birch (*Betula pubescens*) during dormancy cycling.
Lucifer Yellow CH (LYCH) and Fluorescein-tagged GA_4 (F-GA_4) were injected iontophoretically into single cells of the outer cell layer (L_1) of the AM to examine their potential cell–cell transfer via open plasmodesmata.
(a) Dormant AM. Injection with LYCH into a single cell showed that cells (arrow) in the tunica were symplasmically isolated. Insert shows an enlargement of the injected cell with the micro-electrode tip, nucleus (n) and cytoplasm (c). me, micro-electrode.
(b) Dormant AM. Cells were injected individually with F-GA_4 (arrows a and b) or LYCH (arrow c), but neither passed to neighbouring cells. The situation remained unchanged for at least 6 h after injection. me, micro-electrode; p, primordia.
(c) Released but non-proliferating AM (ecodormant). Dormancy has been removed by a chilling period of 6 weeks. LYCH moved from the injected cell to neighbouring cells in a few seconds, revealing the presence of a symplasmic central zone field (czf). Ib, buttress; me, micro-electrode; p, primordia; pz, peripheral zone.
(d) AM as in (c), viewed with a B-filter instead of a BV-filter to block greenish autofluoresence of the surrounding AM areas.
(e) AM as in (c), several hours later (needle removed). The dye-coupling pattern remained the same, indicating closure of plasmodesmata below the SEL for LYCH at the boundary between AM centre and AM periphery.
(f) AM as in (e), viewed with a B-filter instead of a BV-filter to block greenish autofluoresence of the surrounding AM areas.
Imposed regimes for the three AM-stages are indicated in Figure 1. Scale bars: (a,b) 50 μm; (c) 75 μm.

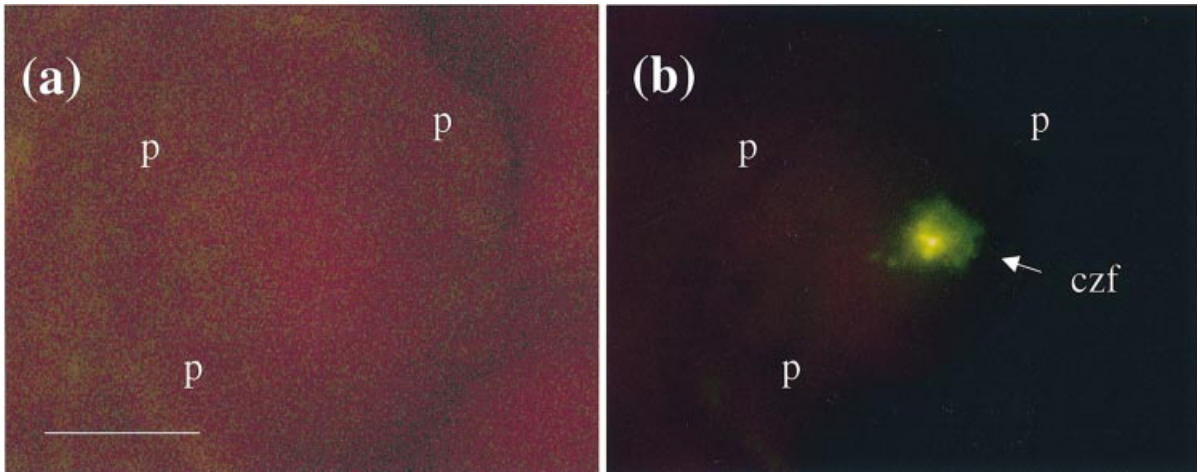

Figure 9. Symplasmic trafficking of Fluorescein-tagged gibberellic acid (F-GA_4) in the shoot apical meristem (AM) of birch (*Betula pubescens*) during dormancy cycling.
(a) Released AM before microinjection showing the position of the primordia.
(b) The same meristem as in (a) after F-GA_4 was iontophoretically injected into a single cell. Cell–cell movement of F-GA_4 was followed under the microscope. F-GA_4 moved to the neighbouring cells in a way similar to LYCH, although somewhat more slowly, demonstrating the opening of the plasmodesmata in the central zone during chilling. F-GA_4 did not open the plasmodesmata between AM centre and periphery during the 6 h after injection. Scale bar: 75 μm; czf, central zone field; p, primordia.

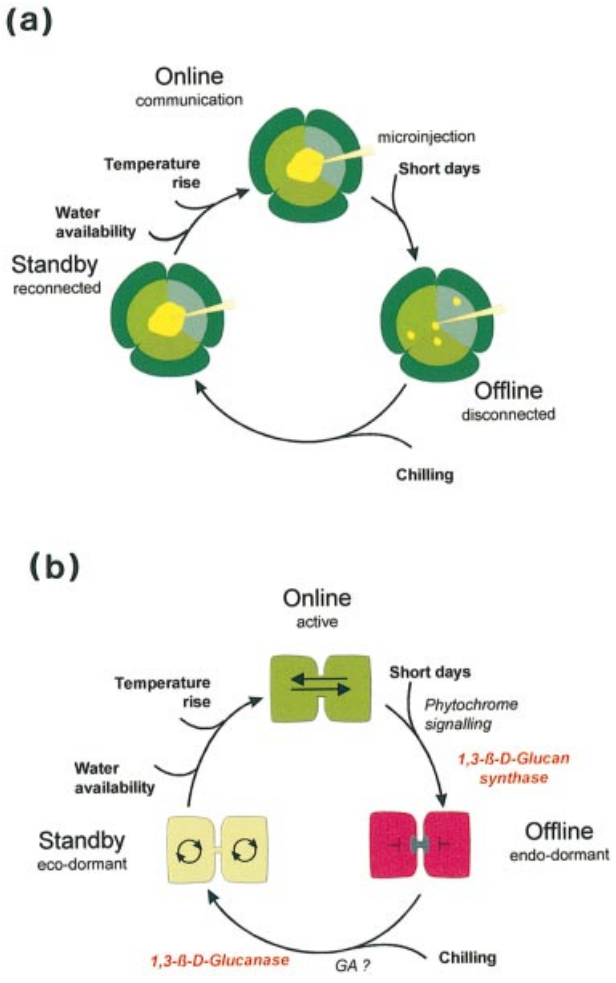

Figure 10. Dormancy cycling in birch (*Betula pubescens*) modelled as an environmentally induced cyclic alteration in the symplasmic communication network of the AM.
(a) Environmental effectors and cell–cell communication patterns in the AM. The AM has a repertoire of at least three distinct and intrinsic symplasmic communication patterns – online, offline and standby – each of which has a unique responsiveness to specific environmental cues (see Figure 1 for conditions). Microinjections of fluorescent dyes show that the actively proliferating AM requires online symplasmic communication via plasmodesmata. Under short days the light-responsive AM switches to an offline state, in which cell–cell communication and photo-responsiveness are suspended. Instead the AM becomes sensitive to chilling, which promotes the formation of a standby state in which the pathways for symplasmic cell–cell communication become restored. Under appropriate conditions, the initiation of cell–cell communication will bring about the online state.
(b) Some cell biological processes involved in the transition in the symplasmic network of the AM. During the online state the AM pre-patterns the shoot in a recurring and oscillatory process (Rinne and van der Schoot, 1998). Under short-day conditions a phytochrome-mediated signal evokes a twofold response of the AM: the production of 1,3-β-D-glucan-containing plasmodesmal sphincters that close the plasmodesmata, and the formation of 1,3-β-D-glucanase containing spherosome-like vacuoles. Initially plasmodesmal closure is reversible, but later it becomes fixed resulting in an offline state (endodormancy). Chilling induces displacement of the 1,3-β-D-glucanase-containing vacuoles towards the peripheral cytoplasm, where they line up at the plasma membrane and associate with plasmodesmal sites. Subsequently, sphincter 1,3-β-D-glucan is digested, and a standby configuration (ecodormant state) emerges. The rise in temperature and the availability of water and nutrients then enhance the physiology of the individual AM cells, leading to an amplification of signal exchange between cells. Eventually, the AM will settle into the collective networking behaviour which is characteristic of morphogenesis.

symplasmic space and partly crosses the extracellular matrix. In the present work we have investigated the organizational changes that occur in the symplasmic space during dormancy cycling, and the putative mechanisms that help enforcing these changes.

Uncoupling the AM cells in response to short photoperiod

Exposure of birch seedlings to short photoperiod leads to formation of plasmodesmal sphincters on all AM cells (Figure 2c), and results in the symplasmic isolation of these cells (Figure 8a,b). The experiments on dormancy cycling were designed to determine whether an explicit correspondence exists between the presence of sphincters and the state of the AM. It appeared that the sphincters, formed under dormancy-inducing conditions, remained present throughout the period of 'true' dormancy, and disappeared when the AM entered ecodormancy, that is, it regained its potential for growth. Apparently the presence of sphincters reflects the state of endodormancy. In TEM sections the relatively translucent sphincters appeared electron-dense when 1% tannic acid was added to the fixative, indicating that they are proteinaceous in nature (Badelt *et al.*, 1994; Olesen and Robards, 1990; Figure 2c). One of the proteins is probably the enzyme 1,3-β-D-glucan synthase, as 1,3-β-D-glucan is deposited locally at the sphincters (Figure 4b,e). Other proteins and non-proteinaceous components may be present, however (Badelt *et al.*, 1994; Turner *et al.*, 1994).

Sphincters are thought to regulate the plasmodesmal size-exclusion limit (SEL) (Olesen and Robards, 1990). A model depicts the enzyme 1,3-β-D-glucan synthase as an integral membrane protein that produces 1,3-β-D-glucan between the plasma membrane and the cell wall (Lucas *et al.*, 1993; Olesen and Robards, 1990). The precise regulation of 1,3-β-D-glucan deposition then fine-tunes the plasmodesmal SEL. Prolonged enzyme activity reduces the inner diameter of the ring, thereby compressing the channel at the neck, eventually resulting in complete closure. In the dormant AM of birch the plasmodesmata are clearly not constricted, however (Figure 2c), yet movement of LYCH and F-GA_4 through the channel is blocked (Figure 8a,b). This is apparently due to the presence of a proteinaceous plug in the plasmodesmal channel, which also contains 1,3-β-D-glucan (Figures 2c, 4e). Plugging of the plasmodesmal channel has been described for *Chara vulgaris*, where it functions in spermatogenesis (Kwiatkowska, 1988). Disparate observations in the literature on channel constriction make it likely that a sphincter ring and a channel plug can form independently, so that a ring alone could function in the fine regulation of the plasmodesmal SEL, as discussed by Olesen and Robards (1990); Badelt *et al.* (1994), whereas the simultaneous formation of a plug, as in the birch AM, would lead to a tight closure of the plasmodesmal channel. The tightness of this closure was apparent when individual cells were impaled with a micro-electrode. The dormant cells osmotically withdraw the dye solution from the electrode tip, resulting in swollen fluorescent cells that did not release the dye for at least a day (Rinne and van der Schoot, 1998).

Reconnecting the AM cells by chilling

In perennial plants, chilling releases buds from dormancy (Coville, 1920) but, paradoxically, it also further enhances the freezing tolerance of the same bud (Rinne *et al.*, 1998). This dual effect becomes comprehensible when chilling is viewed as affecting two different levels of AM organization: dormancy release involves re-establishment of the supracellular organization of the AM (van der Schoot, 1996), whereas freezing tolerance is based on properties of individual AM cells (Rinne *et al.*, 1999).

It is important to note that chilling actually does not activate the dormant AM – which might still experience frost – but unlocks its potential for growth by re-opening the symplasmic communication pathways. Removal of 1,3-β-D-glucan from the plasmodesmata during chilling coincided with the production of 1,3-β-D-glucanase, as demonstrated by Western blots. A 32 kDa 1,3-β-D-glucanase was strongly upregulated after 6 weeks of chilling (Figure 5). *In situ* immunolocalization experiments supported Western blot data in showing that the 1,3-β-D-glucanases were differentially distributed during dormancy cycling. Although in general heterologous antibodies should be used with some caution, the present antibody resulted in a labelling pattern that was specific for the various stages of the AM. In the active AM, 1,3-β-D-glucanases were present mostly at the cell plates of dividing cells (Figure 6a), whereas in the dormant AM they were stored and kept in spherosome-like vacuoles (Figure 6b). Part of such vacuolar 1,3-β-D-glucanase might be processed and active, as in case of tobacco (Sticher *et al.*, 1992). In actively growing plants 1,3-β-D-glucanases function in the removal of extracellular 1,3-β-D-glucan around developing plasmodesmata at the cell plate of dividing cells (Esau, 1977; Kauss, 1996; Verma and Gu, 1996). Our results indicate that 1,3-β-D-glucanases have a similar function during dormancy release in modifying the wall around the plasmodesmata. Chilling induced a shift of 1,3-β-D-glucanase containing vacuoles towards the outer cortical area of the cytoplasm. As a result, most of the spherosome-like vacuoles aligned the plasma membrane, and a substantial number of them were associated with plasmodesmata (Table 1; Figure 2b). Occasionally, vacuoles possessed 1,3-β-D-glucanase-containing extensions towards other plasmodesmata (Figure 7d,e).

The mechanism of plasmodesmal closing and re-opening in the AM has a clear analogy with the phloem of perennials which becomes inactivated in autumn by the deposition of 1,3-β-D-glucan at the sieve-plate pores. The resulting 'dormant' sieve elements become unplugged or re-opened in spring (Esau, 1977) by the activation of 1,3-β-D-glucanase (Krabel *et al.*, 1993). The evolutionary relation between the sieve-plate pores and plasmodesmata – the former are derived from the latter – makes Esau's characterization of plasmodesmata as 'mini-phloem' appropriate (Esau, 1977). Such mini-phloems may be particularly useful in the AM, which does not possess phloem for importation of the necessary materials, to sustain control over vegetative and floral functions. Surprisingly, for phloem the cytological phenomena associated with the functioning of 1,3-β-D-glucanase in the unplugging of the sieve-plate pores have not been investigated.

Origin and nature of 1,3-β-D-glucanase-containing vacuoles

The 1,3-β-D-glucanase-containing vacuoles of birch were surrounded by a 'half-unit' membrane, suggesting that the vacuoles have a spherosome-like nature. Spherosomes originate from the ER under the continuous deposition of triglycerides in the middle layer of their membrane, and as a result the inner side of the membrane gradually shrinks towards the centre of the pro-spherosome and eventually disappears (Matile, 1975). In birch, such inner membrane parts were present in part of the vacuoles (not shown), making it likely that they were indeed derived from the ER. Spherosomes in germinating seeds of pea and bean, similar to those in birch, line up at the plasma membrane prior to germination and disappear soon after (Matile, 1975). Other perennial plants possess lipid-containing 'spherules' that accumulate at the plasma membrane and frequently associate with the plasmodesmata during winter (Pihakaski *et al.*, 1987; Pomeroy and Siminovitch, 1971). These examples suggest that the role of these ER-derived organelles in the release of dormant tissues needs to be addressed further. The present experiments suggest that this type of 'vacuole' has a role in dormancy release. Our finding that they contain 1,3-β-D-glucanases supports early enzyme studies indicating that spherosomes contain hydrolases (Matile, 1975) and have a lysosome-like nature (Gibson and Paleg, 1972; Vigil and Ruddat, 1973). The observed connection between plasmodesmata and the spherosome-like vacuoles could explain the removal of the plasmodesmal sphincters in birch. Spherosomes could digest the sphincters after engulfment (Figure 7c) or, alternatively, they could release hydrolases to the wall sleeve for local sphincter digestion. As we did not find 1,3-β-D-glucanase located precisely inside the plasmodesmata channel or sphincters, the actual mechanism by which the enzymes come into contact with the 1,3-β-D-glucan in the plasmodesmata remains to be established. Nonetheless, our data support the theory of Jones (1976) that plasmodesmata are sites for the release of hydrolytic enzymes into the cell wall.

Gibberellic acid and dormancy release

Although chilling is the natural condition that promotes release from dormancy in many species, application of GA to the bud can substitute for it (Lang, 1957; Purvis, 1961). If endogenous GA plays a role in dormancy release, it has to be produced by the individual AM cells, as all supply routes, symplasmic (Figure 8a,b) and apoplasmic, are closed (Rinne and van der Schoot, 1998). This is in line with earlier observations that chilling effects cannot be imported from other plant parts and that the AM itself must receive chilling (Metzger, 1996). Chilling can activate GA-biosynthetic enzymes locally at the shoot tip (Hazebroek *et al.*, 1993; Zanewich and Rood, 1995), and thus direct chilling of the dormant AM might initiate or enhance GA biosynthesis in individually stimulated cells. This raises the question whether GA – applied or endogenously produced – promotes the production of 1,3-β-D-glucanases. Seed germination studies, for example in tobacco, show that GA_4 activates the transcription of 1,3-β-D-glucanase genes, thereby promoting germination (Leubner-Metzger *et al.*, 1996). This may involve GA-induced degradation of wall material around the plasmodesmata (Jones, 1972). Similarly, GA-induced breakdown of 1,3-β-D-glucan at the plasmodesmata in the AM would allow GA to move from a few starter cells via re-opened plasmodesmata to neighbouring cells, until the entire AM is reconnected. Our experiments with microinjection of F-GA_4 (Figure 9) support earlier observations that GA can move via plasmodesmata (Carr, 1976; Drake and Carr, 1979; Kwiatkowska, 1991). If, however, it is true that GA facilitates reconnection of all AM cells, it may require more than a 6 h period as microinjection of biologically active GA in cells of a dormant AM did not result in cell–cell dye-coupling within this time frame (Figure 8b).

A model of bud dormancy cycling

Supported by these experiments, we have developed a working model for dormancy cycling. During this cycling the AM passes through three sequential states of cell–cell communication: (i) the online state, a proliferative state with physiologically active and dividing cells that continuously exchange matter and information; (ii) the offline state, a state of cellular disconnection and quiescence in which symplasmic cell–cell communication is suspended; and (iii) the standby state, a waiting condition of recon-

nected but inactive cells. The model is based on the observation that the symplasmic communication network, indispensable for AM functioning, is altered specifically by various environmental conditions that drive dormancy cycling (Figure 10). This network model may provide a useful framework for the study of other plant systems that display dormancy–activity cycles.

Experimental procedures

Plant material

Seedlings of birch, *Betula pubescens* Ehrh. (Northern Finnish ecotype, Botanical Garden, University of Oulu, Finland) were grown in 1.2 l pots on a 4 : 1 fertilized mixture (Osmocote, 3 g l^{-1}) of peat and sand under long photoperiod (18 h light; photosynthetic photon flux density 100 μmol m^{-2} sec^{-1}, constant 75% relative humidity, 19°C). Dormancy was initiated by short photoperiod (SD; 8 h light; other conditions as under LD) in 2-month-old seedlings. Dormancy release was investigated by chilling the seedlings for up to 6 weeks at 2°C.

Measurement of bud dormancy and freezing tolerance

Dormancy was assessed after 22 days in bud-burst experiments with single-node cuttings in water culture under growth-promoting forcing conditions, and expressed in a bud-burst index (BB%) (Rinne *et al.*, 1998). Freezing tolerance was monitored with a computer-controlled freezer which cooled at a rate of 2°C h^{-1} down to –30°C (Rinne *et al.*, 1997; Rinne *et al.*, 1998), and subsequently at a rate of 10°C h^{-1} down to –70°C. Stem samples were kept for 1 h at the lowest temperature, then acclimated overnight on an ice bed in a cold room at 4°C. When samples were frozen below –40°C, an additional acclimation step was included and thawing was done after one night at –20°C. Thawed stem samples were cultivated as single-node cuttings growing in water under forcing conditions for a period of 21 days, the time required for freezing injuries to become manifest in dormant buds (Rinne *et al.*, 1998). Bud injuries were assessed with a light microscope according to the method of Ritchie (1991). Freezing tolerance is expressed as the LT_{50} value, denoting the temperature at which 50% of the samples remains uninjured (Rinne *et al.*, 1999).

SDS-PAGE and Western blotting

Proteins were extracted from apical meristems that possessed one or two primordia, separated by discontinuous SDS-PAGE with MINI-PROTEAN II electrophoresis (Bio-Rad, Hercules, CA, USA), electroblotted, and immunodetected as described earlier (Rinne *et al.*, 1998; Welling *et al.*, 1997). In short, six meristems were isolated under the stereomicroscope (Nikon, Tokyo, Japan), grounded on 30 μl Towbin loading buffer (Towbin *et al.*, 1979), and directly loaded onto two gels. One of the gels was stained with Coomassie Brilliant Blue G-250 (Neuhoff *et al.*, 1988) to check the amounts of loaded protein. Proteins from unstained parallel gels were immunoblotted onto 0.2 μm nitrocellulose membranes (Bio-Rad). Membranes were incubated with 1 : 1000 diluted polyclonal antibody raised against stress-inducible 1,3-β-D-glucanases of tobacco (provided by P. de Wit, Wageningen Agricultural University, The Netherlands). The polyclonal antibody recognizes both class I (vacuolar) and class II (secreted) 1,3-β-D-glucanases (P. de Wit, personal communication). Western blots were examined for possible cross-reactivity with the non-immune rabbit serum (Sigma). Goat anti-rabbit IgG alkaline phosphatase conjugate (Sigma) and a substrate kit (Bio-Rad) were subsequently used for detection of the 1,3-β-D-glucanases.

Light and transmission electron microscopy

For LM and TEM, apices were fixed for 4 h in 2% (v/v) glutaraldehyde in 100 mM phosphate buffer (pH 7.2), with or without 1% (w/v) tannic acid, post-fixed for 2 h in 1% (w/v) OsO_4, and embedded in Spurr's resin (Sigma) (Rinne and van der Schoot, 1998). Median longitudinal sections (1–4 μm thick) were stained either with 1% Toluidine Blue or with a combination of Methylene Blue, Azure and Basic Fuchsin (Clark, 1981), and investigated microscopically (Nikon Optiphot 2). Ultra-thin sections (70 nm) were cut from the AM with an ultramicrotome (Leica, Nestzlar, Germany), stained with 2% aqueous uranyl acetate and Reynolds' lead citrate, and examined with a JEOL 1200 EXII electron microscope at 80 kV (Tokyo, Japan).

Immunogold labelling

Apices were fixed for 4 h in a mixture of 0.75% (v/v) glutaraldehyde, 1.6% (w/v) paraformaldehyde and 0.75% (v/v) acrolein, in 50 mM phosphate buffer (pH 7.2) and embedded in LR White resin (Agar Scientific, Stansted, Essex, UK). Sections were blocked for 1 h in a solution of 0.8% BSA, 0.1% gelatin and 5% normal goat serum in phosphate-buffered saline (10 mM Na_2HPO_4/NaH_2PO_4 and 150 mM NaCl) pH 7.4. Sections were incubated for 1 h in 1 : 500 diluted anti-1,3-β-D-glucanase antibodies or anti-1,3-β-D-glucan antibodies (Gensys Biotechnologies Inc, UK, Cambridge, UK). A blocking solution with 1% normal goat serum was used for washing and incubation with antibodies. Immunoreactivity was visualized by a 1 h incubation with goat anti-rabbit antibodies linked to colloidal gold particles (1 and 10 nm; Amersham Pharmacia Biotech Ltd, Bucks, UK). Gold particles (1 nm) were silver-enhanced for 10 min at room temperature and examined by LM. Immunolabelling was repeated several times in three independent embeddings. Specificity of the labelling was assessed by omitting the primary antibody, by using unrelated antibodies, and by using non-immune serum (Sigma). Sections were examined and photographed with LM or TEM. The extent of plasmodesmal labelling was assessed by counting gold label in the TEM, and expressing it as the average number of gold particles per plasmodesma. The counts were analysed by statistical software (ANOVA, SIGMABLOT for Windows).

Electrophysiology and dye coupling

Iontophoresis and electrophysiology were performed as described by Rinne and van der Schoot (1998); Storms *et al.* (1998). In short, the exposed AM (on 3 mm stem) was positioned upright in a bathing chamber that was filled with medium or tap water at 20°C. After 0.5 h the AM surface was inspected under low-irradiance white light. The extent of green autofluorescence of cut leaves was assessed by short epi-illumination with blue-violet (BV) and blue (B) light in a fluorescence microscope (Nikon Optiphot 2). Excitation and barrier filters were as described previously (Rinne and van der Schoot, 1998). Adjacent, undamaged leaf primordia could also show some greenish autofluores-

cence (Figure 8c,e), albeit weaker than damaged leaves. The undamaged AM was commonly free of green autofluorescence, and appeared red due to chlorophyll fluorescence (Figure 8a). A sharp drop in the recorded electrical potential signalled microelectrode entry into a tunica cell. After the recording of a stable membrane potential, Lucifer Yellow CH or Fluorescein-tagged GA_4 (Pulici *et al*., 1996) was injected with low, intermittent current (–1 to –5 nA) into the target cell, and the spread to other cells was monitored and recorded on Ektachrome 400 super slide film.

Acknowledgements

The authors thank Pierre de Wit for a gift of anti-1,3-β-D-glucanase antibodies, Tadeo Asuki for Fluorescein-tagged GA_4, Koos Oosterhaven and Rob Goldbach for support, Klaus-Peter Krause and Oscar Goddijn for helpful discussions and input to Figure 10, Trygve Krekling and Elisabeth Reed Eng for use of TEM facilities, Annikki Welling for providing plant material, Raili Ruonala for preparation of TEM samples, and the personnel of the Botanical Gardens of the University of Oulu for taking care of the plants. We thank the anonymous reviewers for helpful comments. The Academy of Finland is acknowledged for financial support to P.R. (grants 44914, 51350).

References

Badelt, K., White, R.G., Overall, R.L. and Vesk, M. (1994) Ultrastructural specializations of the cell wall sleeve around plasmodesmata. *Am. J. Bot.* **81**, 1422–1427.

Bergmans, A., de Boer, D., van Bel, A. and van der Schoot, C. (1993) The initiation and development of *Iris* flowers: permeability changes in the apex symplasm. *Flowering Newsl.* **16**, 19–26.

Bergmans, A.C.J., de Boer, A.D., Derksen, J.W.M. and van der Schoot, C. (1997) The symplasmic coupling of L_2-cells diminishes in early floral development of *Iris*. *Planta*, **203**, 245–252.

Bewley, J.D. (1997) Seed germination and dormancy. *Plant Cell*, **9**, 1055–1066.

Bianco, J., Lassechere, S. and Polard, C. (1984) Gibberellins in dormant embryos of *Pyrus malus* L. cv. Golden Delicious. *J. Plant. Physiol.* **116**, 185–188.

Carr, D.J. (1976) Plasmodesmata in growth and development. In *Intercellular Communication in Plants: Studies on Plasmodesmata* (Gunning, B.E.S. and Robards, A.W., eds). Berlin, Heidelberg, New York: Springer, pp. 243–289.

Clark, G. (1981) *Staining Procedures*. London: Williams & Wilkins.

Cohn, M.A. (1996) Chemical mechanisms of breaking seed dormancy. In *Plant Dormancy. Physiology, Biochemistry and Molecular Biology* (Lang, G.A., ed.). Wallingford, UK: CAB International, pp. 257–265.

Coville, F.V. (1920) The influence of cold in stimulating the growth of plants. *J. Agric. Res.* **20**, 151–160.

Crawford, K.M. and Zambryski, P.C. (1999) Plasmodesmata signaling: many roles, sophisticated statutes. *Curr. Opin. Plant Biol.* **2**, 382–387.

Drake, G.A. and Carr, D.J. (1979) Symplastic transport of gibberellins: evidence from flux and inhibitor studies. *J. Exp. Bot.* **116**, 439–447.

Esau, K. (1977). *Anatomy of Seed Plants*, 2nd edn. New York: John Wiley.

Gassner, G. (1918) Beiträge zur physiologischen Charakteristik sommer-und winterannueller Gewächse insbesondere der Getreidepflanzen. *Z. Bot.* **10**, 417–430.

Gibson, R.A. and Paleg, L.G. (1972) Lysosomal nature of hormonally induced enzymes in wheat aleurone cells. *Biochem. J.* **128**, 367–375.

Gisel, A., Barella, S., Hempel, F.D. and Zambryski, P.C. (1999) Temporal and spatial regulation of symplastic trafficking during development in *Arabidopsis thaliana* apices. *Development*, **126**, 1879–1889.

Hauser, B.A., Cordonnier-Pratt, M.-M. and Pratt, L.H. (1998) Temporal and photoregulated expression of five tomato phytochrome genes. *Plant J.* **14**, 431–439.

Hazebroek, J.P., Metzger, J.D. and Mansager, E.R. (1993) Thermoinductive regulation of gibberellin metabolism in *Thlaspi arvense* L. II. Cold induction of enzymes in gibberellin biosynthesis. *Plant Physiol.* **102**, 547–552.

Jones, M.G.K. (1976) The origin and development of plasmodesmata. In *Intercellular Communication in Plants: Studies on Plasmodesmata* (Gunning, B.E.S. and Robards, A.W., eds). Berlin, Heidelberg, New York: Springer, pp. 81–105.

Jones, R.L. (1972) Fractionation of the enzyme of the barley aleurone layer: evidence for a soluble mode of enzyme release. *Planta*, **103**, 95–109.

Kauss, H. (1996) Callose synthesis. In *Membranes: Specialized Functions in Plants* (Smallwood, M., Knox, J.P. and Bowles, D.J., eds). UK: Bios Scientific Publishers, pp. 77–92.

Kircher, S., Kozma-Bognar, L., Kim, L., Adam, E., Harter, K., Schäfer, E. and Nagy, F. (1999) Light quality-dependent nuclear import of the plant photoreceptors phytochrome A and B. *Plant Cell*, **11**, 1445–1456.

Krabel, D., Eschrich, W., Wirth, S. and Wolf, G. (1993) Callase-(1,3-beta-D-glucanase) activity during spring reactivation in deciduous trees. *Plant Sci.* **93**, 19–23.

Kwiatkowska, M. (1988) Symplasmic isolation of *Chara vulgaris* antheridium and mechanisms regulating the process of spermatogenesis. *Protoplasma*, **142**, 137–146.

Kwiatkowska, M. (1991) Autoradiographic studies on the role of plasmodesmata in the transport of gibberellin. *Planta*, **183**, 294–299.

Lang, A. (1957) The effect of gibberellin upon flower formation. *Proc. Natl Acad. Sci. USA*, **43**, 709–711.

Lang, G.A. (1987) Dormancy: a new universal terminology. *Hortscience*, **22**, 817–820.

Lang, G.A. (1994) Dormancy – the missing links: molecular studies and integration of regulatory plant and environmental interactions. *Hortscience*, **29**, 1255–1263.

Lang, G.A. (1996) *Plant Dormancy. Physiology, Biochemistry and Molecular Biology*. Wallingford, UK: CAB International.

Laufs, P., Jonak, C. and Traas, J. (1998a) Cells and domains: two views of the shoot apical meristem in *Arabidopsis*. *Plant Physiol. Biochem.* **36**, 33–45.

Laufs, P., Grandjéan, O., Jonak, C., Kiêu, K. and Traas, J. (1998b) Cellular parameters of the shoot apical meristem in *Arabidopsis*. *Plant Cell*, **10**, 1375–1389.

Lenhard, M. and Laux, T. (1999) Shoot meristem formation and maintenance. *Curr. Opin. Plant Biol.* **2**, 44–50.

Leubner-Metzger, G., Fründt, C. and Meins, F., Jr (1996) Effects of gibberellins, darkness and osmotica on endosperm rupture and class I β-1,3-glucanase induction in tobacco seed germination. *Planta*, **199**, 282–288.

Lucas, W.J., Ding, B. and van der Schoot, C. (1993) Plasmodesmata and the supracellular nature of plants. *New Phytol.* **125**, 435–476.

Matile, Ph. (1975). *The Lytic Compartment of Plant Cells*. Wien: Springer.

McLean, B.G., Hempel, F.D. and Zambryski, P.C. (1997) Plant intercellular communication via plasmodesmata. *Plant Cell*, **9**, 1043–1054.

Metzger, J.D. (1988) Localisation of the site of perception of thermoinductive temperatures in *Thlaspi arvense* L. *Plant Physiol.* **88**, 424–428.

Metzger, J.D. (1996) A physiological comparison of vernalization and dormancy chilling requirement. In *Plant Dormancy. Physiology, Biochemistry and Molecular Biology* (Lang, G.A., ed.). Wallingford, UK: CAB International, pp. 147–155.

Meyerowitz, E.M. (1999) Plants, animals and the logic of development. *Trends Cell Biol*. **9**, 65–68.

Neuhoff, V., Arold, N., Taube, D. and Ehrhardt, W. (1988) Improved staining of proteins in polyacrylamide gels including isoelectric focusing gels with clear background at nanogram sensitivity using Coomassie Brilliant Blue G-250 and R-250. *Electrophoresis*, **9**, 255–262.

Noodén, L.D. and Weber, J.A. (1978) Environmental and hormonal control of dormancy in terminal buds of plants. In *Dormancy and Developmental Arrest. Experimental Analysis in Plants and Animals* (Cutter, M.E., ed.). New York: Academic Press, pp. 221–268.

Olesen, P. and Robards, A.W. (1990) The neck region of plasmodesmata: general architecture and some functional aspects. In *Parallels in Cell to Cell Junctions in Plants and Animals* (Robards, A.W., Lucas, W.J., Pitts, J.D., Jongsma, H.J. and Spray, D.C., eds). Berlin: Springer, pp. 145–170.

Pihakaski, K., Pihakaski, S., Karunen, P. and Kallio, P. (1987) Seasonal changes in leaf lipids of *Diapensia lapponica*, with special reference to storage lipid bodies. *Nord. J. Bot.* **7**, 281–292.

Pomeroy, M.K. and Siminovitch, D. (1971) Seasonal cytological changes in secondary phloem parenchyma cells in *Robinia pseudoacacia* in relation to cold hardiness. *Can J. Bot.* **49**, 787–795.

Powell, L.E. (1987) The hormonal control of bud and seed dormancy in woody plants. In *Plant Hormones and their Role in Plant Growth and Development* (Davies, P.J., ed.). Dordrecht: Martinus-Nijhoff, pp. 539–552.

Pulici, M., Asami, T., Robertson, M., Seto, H. and Yoshida, S. (1996) Amylase induction activity of fluorescein labeled gibberellin in barley aleurone protoplasts. *Bioorg. Med. Chem. Lett.* **6**, 2549–2552.

Purvis, O.N. (1940) Vernalization of fragments of embryo tissues. *Nature*, **145**, 462.

Purvis, O.N. (1961) The physiological analysis of vernalization. *Encycl. Plant Physiol.* **16**, 76–122.

Rinne, P.L.H. and van der Schoot, C. (1998) Symplasmic fields in the tunica of the shoot apical meristem coordinate morphogenetic events. *Development*, **125**, 1477–1485.

Rinne, P., Hänninen, H., Kaikuranta, P., Jalonen, J.E. and Repo, T. (1997) Freezing exposure releases bud dormancy in *Betula pubescens* and *B. pendula*. *Plant Cell Environ.* **20**, 1199–1204.

Rinne, P., Welling, A. and Kaikuranta, P. (1998) Onset of freezing tolerance in birch (*Betula pubescens* Ehrh.) involves LEA proteins and osmoregulation and is impaired in an ABA-deficient genotype. *Plant Cell Environ.* **21**, 601–611.

Rinne, P.L.H., Kaikuranta, P.L.M., van der Plas, L.H.W. and van der Schoot, C. (1999) Dehydrins in cold acclimated apices of birch (*Betula pubescens* Ehrh.): production, localization and potential role in rescuing enzyme function during dehydration. *Planta*, **209**, 377–388.

Ritchie, G.A. (1991) Measuring cold hardiness. In *Techniques and Approaches in Forest Tree Ecophysiology* (Lassoie, J.P. and Hinckley, T.M., eds). Boca Raton, FL: CRC Press, pp. 557–582.

Romberger, J.A. (1963) Meristems, growth and development in woody plants. *USDA Techn. Bull.* **1293**.

Salisbury, F.B. and Ross, C.W. (1992) *Plant Physiology*. Belmont, California: Wadsworth Publishing Co.

Shirazi, A.M. and Fuchigami, L.H. (1995) Effects of 'near-lethal' stress on bud dormancy and stem cold hardiness in red-osier dogwood. *Tree Physiol.* **15**, 275–279.

Sticher, L., Hinz, U., Meyer, A.D. and Meins, F., Jr (1992) Intracellular transport and processing of a tobacco vacuolar β-1,3-glucanase. *Planta*, **188**, 559–565.

Storms, M.M.H., van Schoot, C., Prins, M., Kormelink, R., van Lent, J.W.M. and Goldbach, R.W. (1998) A comparison of two methods of microinjection for assessing altered plasmodesmal gating in tissues expressing viral movement proteins. *Plant J.* **13**, 131–140.

Tanino, K.K., Fuchigami, L.H., Chen, T.H.H., Gusta, L.V. and Weiser, C.J. (1989) Dormancy-breaking agents on acclimation and deacclimation of dogwood. *Hortscience*, **24**, 353–354.

Towbin, H., Staehelin, T. and Cordon, J. (1979) Electrophoretic transfer of proteins from polyacrylamide gels to nitrocellulose sheets: procedure and some applications. *Proc. Natl Acad. Sci. USA,* **76**, 4350–4354.

Turner, A., Wells, B. and Roberts, K. (1994) Plasmodesmata of maize root tips: structure and composition. *J. Cell Sci.* **107**, 3351–3361.

van der Schoot, C. (1996) Dormancy and symplasmic networking at the shoot apical meristem. In *Plant Dormancy. Physiology, Biochemistry and Molecular Biology* (Lang, G.A., ed.). Wallingford, UK: CAB International, pp. 59–81.

van der Schoot, C. and Rinne, P. (1999a) The symplasmic organization of the shoot apical meristem of angiosperms. In *Plasmodesmata: Structure, Function, Role in Cell Communication* (van Bel, A.J.E. and van Kesteren, W.J.P., eds) Dordrecht: Springer, pp. 225–242.

van der Schoot, C. and Rinne, P. (1999b) Networks for shoot design. *Trends Plant Sci.* **4**, 31–37.

Vegis, A. (1964) Dormancy in higher plants. *Annu. Rev. Plant Physiol.* **15**, 185–224.

Verma, D.P.S. and Gu, X. (1996) Vesicle dynamics during cell-plate formation in plants. *Trends Plant Sci.* **1**, 145–149.

Vernoux, T., Autran, D. and Traas, J. (2000) Developmental control of cell division patterns in the shoot apex. *Plant Mol. Biol.* **40**, 569–581.

Vigil, E.L. and Ruddat, M. (1973) Effect of gibberellic acid and actinomycin D on the formation and distribution of rough endoplasmic reticulum in barley aleurone cells. *Plant Physiol.* **51**, 549–558.

Vince-Prue, D. (1994) The duration of light and photoperiodic responses. In *Photomorphogenesis in Plants* (Kendrick, R.E. and Kronenberg, G.H.M., eds). 2nd edn. Dordrecht: Kluwer Academic, pp. 447–490.

Walker, D.R. and Donoho, C.W. (1959) Further studies on the effect of gibberellic acid on breaking the rest period of young peach and apple trees. *Proc. Am. Soc. Hort. Sci.* **74**, 87–92.

Weiser, C.J. (1970) Cold resistance and injury in woody plants. *Science*, **169**, 1269–1278.

Welling, A., Kaikuranta, P. and Rinne, P. (1997) Photoperiodic induction of dormancy and freezing tolerance in *Betula pubescens*. Involvement of ABA and dehydrins. *Physiol. Plant.* **100**, 119–125.

Wisniewski, M., Fuchigami, L.H., Sauter, J.J., Shirazi, A. and

Zhen, L. (1996) Near-lethal stress and bud dormancy in woody plants. In *Plant Dormancy. Physiology, Biochemistry and Molecular Biology* (Lang, G.A., ed.). Wallingford, UK: CAB International, pp. 201–210.

Yamaguchi, R., Nakamura, M., Mochizuki, N., Kay, S.A. and Nagatani, A. (1999) Light-dependent translocation of a phytochrome B-GFP fusion protein to the nucleus in transgenic *Arabidopsis*. *J. Cell Biol.* **145**, 437–445.

Zanewich, K.P. and Rood, S.B. (1995) Vernalization and gibberellin physiology of winter carnola: endogenous gibberellin (GA) content and metabolism of [^{3}H]GA_1, and [^{3}H]GA_{20}. *Plant Physiol.* **108**, 615–621.